Discharge Oscillations in a Permanent Magnet Cylindrical Hall-Effect Thruster

IEPC-2009-122

Presented at the 31st International Electric Propulsion Conference, Ann Arbor, MI
September 20-24, 2009

K.A. Polzin* and E.S. Sooby†
NASA-Marshall Space Flight Center, Huntsville, AL 35812

Y. Raitses‡ E. Merino and N.J. Fisch§
Princeton Plasma Physics Laboratory, Princeton, NJ 08543

Measurements of the discharge current in a cylindrical Hall thruster are presented to quantify plasma oscillations and instabilities without introducing an intrusive probe into the plasma. The time-varying component of the discharge current is measured using a current monitor that possesses a wide frequency bandwidth and the signal is Fourier transformed to yield the frequency spectra present, allowing for the identification of plasma oscillations. The data show that the discharge current oscillations become generally greater in amplitude and complexity as the voltage is increased, and are reduced in severity with increasing flow rate. The 'breathing' mode ionization instability is identified, with frequency as a function of discharge voltage not increasing with discharge voltage as has been observed in some traditional Hall thruster geometries, but instead following a scaling similar to a large-amplitude, nonlinear oscillation mode recently predicted in for annular Hall thrusters. A transition from lower amplitude oscillations to large relative fluctuations in the oscillating discharge current is observed at low flow rates and is suppressed as the mass flow rate is increased. A second set of peaks in the frequency spectra are observed at the highest propellant flow rate tested. Possible mechanisms that might give rise to these peaks include ionization instabilities and interactions between various oscillatory modes.

I. Introduction

PLASMA oscillations are ubiquitous in Hall thrusters,[1] where many different plasma wave modes are supported by the electric and magnetic field topologies present. Various oscillatory plasma processes can also be inherent in the operation of the thruster, serving to set the upper limits on thruster performance by controlling the ionization and acceleration processes within the discharge channel.

The cylindrical Hall thruster[2] (CHT) combines characteristics of both the end-Hall thruster[3] (EHT) and the conventional (annular) stationary plasma thrusters[4] (SPT). Although conventional Hall thrusters can operate at high thrust efficiency at kilowatt power levels, it is difficult to construct one that operates over a broad power envelope down to $\mathcal{O}(100$ W) while maintaining relatively high efficiency.[5] Scaling to low power requires a decrease in the thruster channel size and an increase in the magnetic field strength while holding the dimensionless performance scaling parameters constant.[4,6] Increasing the magnetic field becomes technically challenging because the field can more easily saturate the miniaturized inner components of the magnetic circuit, and scaling down the magnetic circuit leaves very little room for magnetic pole pieces and heat shields.

*Propulsion Research Engineer, Propulsion Research and Technology Applications Branch, Propulsion Systems Department. kurt.a.polzin@nasa.gov

†Undergraduate Intern; currently IGERT Applied Science Research Fellow, Texas A&M University, College Station, TX.

‡Research Physicist.

§Professor, Astrophysical Sciences Dept.

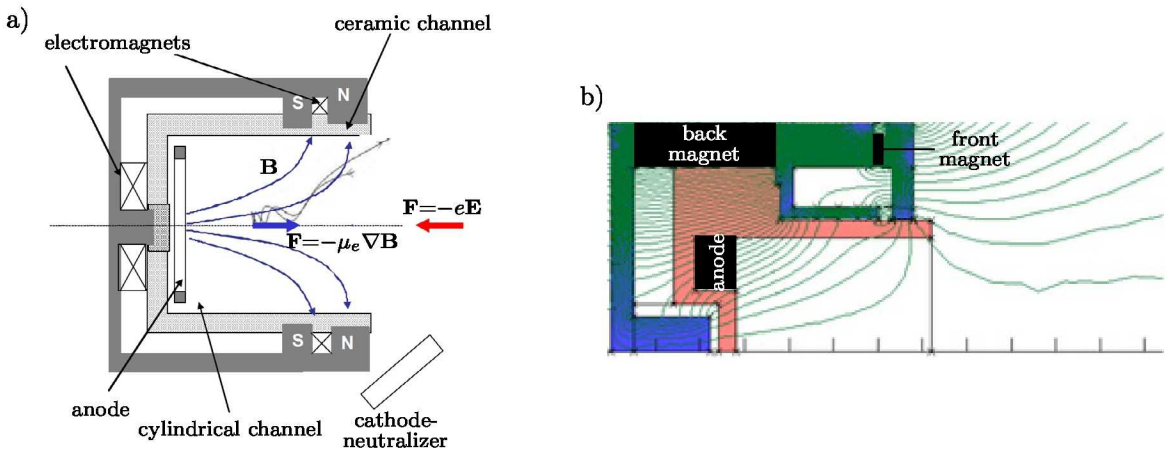

Figure 1. a) Schematic of a cylindrical Hall thruster (CHT) showing the general magnetic field topology produced by electromagnets. b) Magnetic field topology in a laboratory model 2.6 cm CHT with Sm-Co permanent magnets where the magnets are oriented in a direct-field alignment. The maximum magnetic field is roughly 1 kG at the axis near the back wall.

An alternative approach to the miniaturization problem that has been demonstrated is embodied in the CHT, which is shown schematically in Fig. 1a. In contrast to the conventional annular geometry, in the cylindrical geometry the axial potential distribution is critical for electron confinement. This is because there is a large axial gradient in the magnetic field in the channel. The electrons drift both azimuthally around the thruster axis and outwards through the $\mu_e \nabla B$ force. In the absence of an axial potential, the electrons would mirror out of the region of high magnetic field. In the CHT, the axial potential that accelerates ions outwards also plays an important role in confining the electrons within the thruster by counteracting the mirroring effect.

The electric and magnetic field topologies of the CHT are significantly more complex than that found in the annular Hall thruster. The magnetic field is mostly radial at the outer diameter of the discharge channel exit and mostly axial at the thruster back-end. Furthermore, if we assume the equipotential surfaces match the magnetic field contours, then the electric field can have a two-dimensional profile that is just as complex as the magnetic field. The field structure in a CHT may not only support a variety of plasma waves and instabilities, but also lead to waves that have a much greater spectral range compared to what has been measured in conventional Hall thrusters.

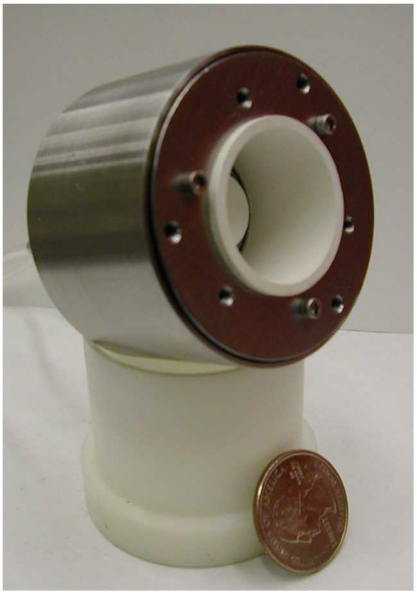

Figure 2. Laboratory model 2.6 cm CHT with Sm-Co permanent magnets (with US quarter for scale).

In this work, oscillations in the discharge current are measured and used to identify and quantify waves and oscillations in a CHT (see Refs. [7–11] for experimental and theoretical examples of this technique applied to an SPT geometry). As a result, this method is not capable of identifying waves and instabilities that do not result in discharge current fluctuations. However, it also will not excite additional waves and oscillations in an otherwise quiescent plasma as can occur through direct probing of a plasma. We present discharge current data and then Fourier transform these data to expose the frequency spectrum present at different operating conditions. The observed oscillations and instabilities are discussed in the context of previous measurements and theoretical treatments of oscillations in annular Hall thrusters.

II. Experimental Apparatus

Tests were conducted on a cylindrical Hall thruster at NASA's Marshall Space Flight Center (MSFC). We proceed first with a description of the thruster and then discuss the facilities and test equipment at MSFC.

A. Cylindrical Hall Thruster with Permanent Magnets

Measurements were obtained using the 2.6 cm channel diameter permanent magnet Princeton Plasma Physics Laboratory (PPPL) CHT shown in Fig. 2. The thruster is roughly 5.5 cm in overall diameter and 3.5 cm long, massing roughly 350 g. The thruster channel is comprised of a ceramic boron-nitride insulator with propellant fed from an annular anode. Two sets of samarium-cobalt (Sm-Co) rare-Earth ring magnets are used to produce the magnetic field. The magnets in this case are oriented in the same direction to produce a 'direct' magnetic field topology, as shown in Fig. 1b. The maximum field strength inside the thruster channel is roughly 1 kG.

B. NASA-MSFC Test Facility

Testing at NASA-MSFC was conducted in a 2.75-m diameter, 7.6-m long stainless steel vacuum chamber. Testing of a different PPPL CHT has been previously performed in this facility.[12] The vacuum level inside the chamber is maintained by two 9500 l/s gaseous helium cryopumps. The base pressure of the facility was 2×10^{-7} torr, and the pressure level during testing was roughly 1×10^{-5} torr.

The working propellant for all experiments is research-grade xenon gas. A commercial HeatWave Labs HWPES-250 hollow cathode is used in these experiments, serving as both the thruster cathode and the beam neutralizer. The propellant flow rate to the cathode and anode were independently controlled using two variable 10-sccm MKS 1479 precision flow controllers (calibrated on Xe and controllable to ±0.1 sccm). All testing was performed with a cathode flow rate of 2 sccm.

Discharge oscillation data were obtained using a Pearson Electronics current monitor (model 2877). This monitor has a frequency bandwidth from 300 Hz to 200 MHz. It does not measure DC current levels, so the output signal is composed entirely of oscillatory current components. Previous experiments with magnetoplasmadynamic thrusters have exhibited current and voltage oscillations due not to the thruster physics but rather the natural oscillations and dispersion within the transmission line and power supply.[13] The effects of any transmission line modes and resonances were minimized in our experiments by placing the current monitor around the wire feeding power to the anode at a location as close to the thruster as possible.

An additional diagnostic employed in these experiments was a Tektronix P5210 100/1000x differential voltage probe. It is capable of measuring voltages up to 4400 V and has a bandwidth of 50 MHz. The probe was located inside the vacuum chamber, directly measuring the voltage between the cathode and anode. These data are not presented in this paper because it was found that the discharge voltage variation was relatively insignificant (less than $\pm1\%$ of the applied voltage).

III. Experimental Data

Discharge current waveforms are presented in Figs. 3 and 4 for a variety of operating conditions. These data are comprised of the sum of the time-varying, oscillatory component measured using the current monitor and the average, DC value of the current output by the power supply. The time-varying current components in these figures were obtained at a sampling rate of 1 μs/point or 1 MHz. The operating conditions were varied to include four discharge voltages (200, 250, 300, and 350 V) and three anode flow rates (3.4, 4.4, and 5.0 sccm Xe). While the data in the 3.4 sccm case exhibits a very regular oscillatory pattern, a longer timespan is used in presenting the 4.4 and 5.0 sccm data (Fig. 3(right side) and 4, respectively) so as to expose not only the shorter-term oscillations but also a longer-term modulation that appears in these waveforms.

The frequency spectra of the current waveforms found in Figs. 3 and 4 are presented in Fig. 5a-c. In the figures, these data span a range from 6 kHz to 100 kHz. In addition, current waveform frequency spectra obtained for the 5.0 sccm case measured at a sampling rate of 100 kHz are presented in Fig. 5d. These data are shown over the range of 6 kHz to 50 kHz, and are presented to reveal more spectral detail at the lower

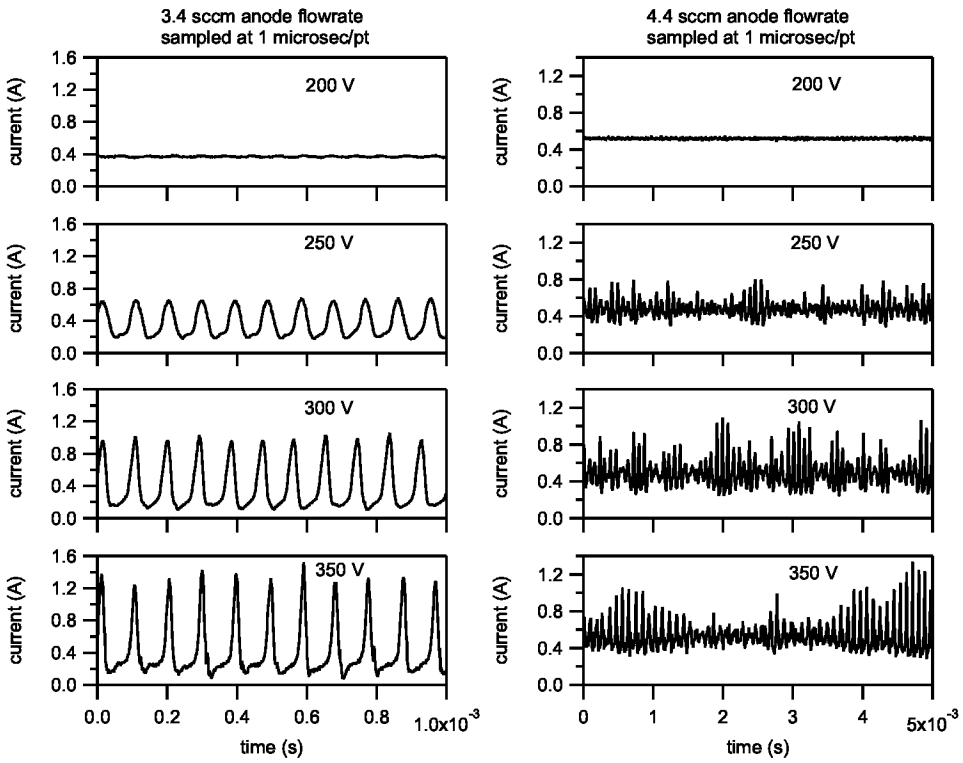

Figure 3. Discharge current as a function of time for a flow rate of 3.4 sccm Xe (left side) and 4.4 sccm Xe (right side) showing the time-varying nature of the current waveform at different discharge voltages.

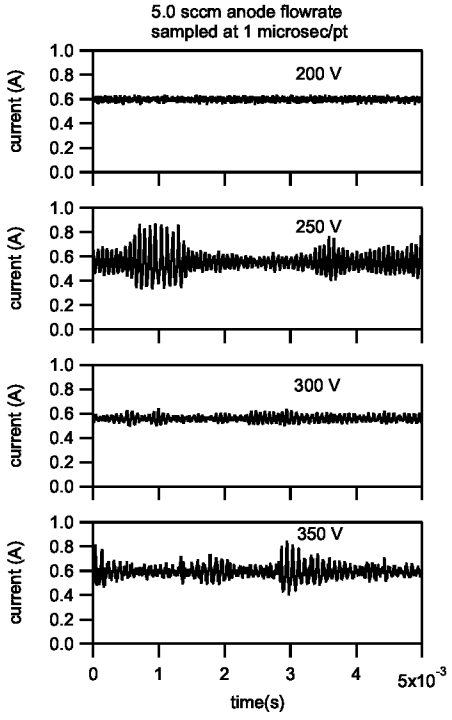

Figure 4. Discharge current as a function of time for a flow rate of 5.0 sccm Xe showing the time-varying nature of the current waveform at different discharge voltages.

frequencies. In all cases, a fast Fourier transform was only performed on the time-varying component of the measured current, and the output represents the resulting magnitude of the Fourier transform.

IV. Observations & Discussion

Observations on the data presented in the previous section reveal the presence of many interesting features. At 3.4 sccm (Fig. 3-left side), the oscillatory nature of the waveform is obviously not purely sinusoidal, and the low point in the oscillation is closer to zero current as the voltage is increased. At 4.4 and 5.0 sccm (Fig. 3-right side and Fig. 4, respectively), the low point in the oscillations is well above the zero current level. For these two flow rates, as the discharge voltage is increased the oscillations that appear at 3.4 sccm are additionally modulated by a second, lower frequency signal. This modulation is generally more pronounced at greater discharge voltage levels. The average discharge current for each case found in Figs. 3 and 4 is shown in Fig. 6a-c. These graphs include both the standard deviation of the current waveform, shown using vertical bars, and the minimum and maximum extents of the current waveform, shown using open triangles. In general, the oscillatory responses observed in the current data are greater as the discharge voltage is increased and are reduced in magnitude for higher anode flow.

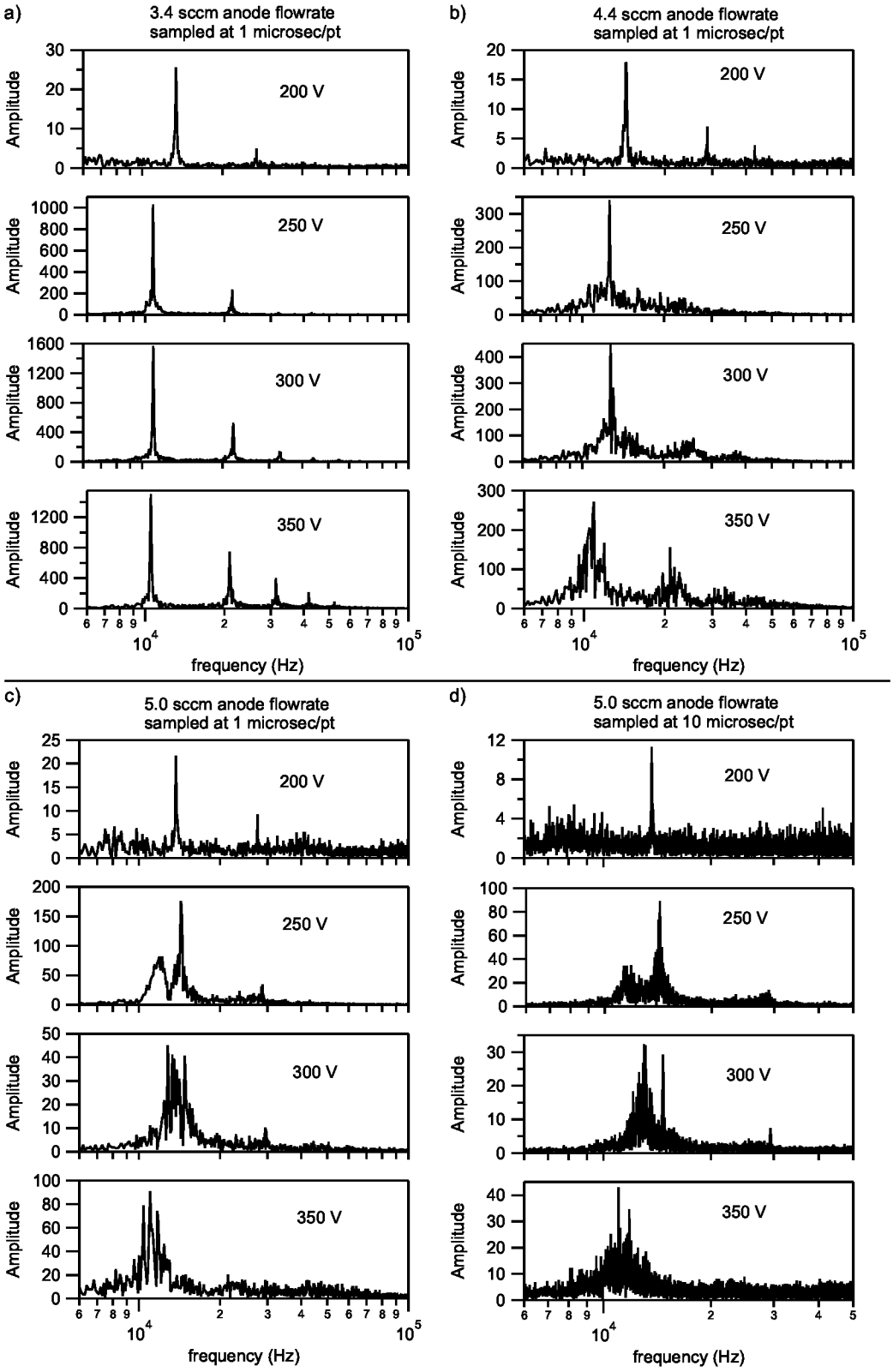

Figure 5. Results of a Fast Fourier Transform of the discharge current for different discharge voltages obtained at a flow rate of 3.4 sccm Xe (section a), 4.4 sccm Xe (section b), and 5.0 sccm Xe sampled at a rate of 1 μs/point (section c) and 10 μs/point (section d).

In all the frequency spectra (Fig. 5) there exists a fundamental frequency oscillation and at several operating points there are higher frequency harmonics, though these harmonics are more difficult to observe in some data sets because they are small relative to the overall fluctuations in the frequency spectrum data. At flow rates of 3.4 and 4.4 sccm, the fundamental oscillatory frequency is very well defined, and at higher discharge voltages the number of higher frequency harmonics and the power present in those harmonics increase. The width of the peaks increase at greater propellant flow rates. At 5.0 sccm additional, broad-width features in the frequency spectra appear (in the 11-14 kHz range) and grow in amplitude relative to the fundamental oscillating frequency as the voltage is increased. In fact, these oscillations are so large in magnitude and broad in frequency that the fundamental frequency in the 350 V data cannot be accurately determined. The frequency spectra in Fig. 5d were acquired at a slower speed to provide a better frequency-domain resolution of these features and show that there were indeed two separate structures being observed. These are not additional harmonics of the fundamental oscillation observed in the other data sets, but instead represent an entirely different feature in the data.

At a discharge voltage of 200 V the data exhibit noticeable differences relative to the other voltages. For flow rates of 3.4 and 4.4 sccm, the peak in the fundamental frequency harmonic at 200 V is located at a higher frequency than for the other voltages, and as expected the frequency spectra show that the amplitude of these oscillations and harmonics are much lower than for the other discharge voltage levels. In addition, previously published thrust stand measurements[14] reveal that this particular thruster possesses an anode thrust efficiency that is significantly reduced when operating below 250 V. All these data imply that the thruster is operating in a different mode at the lower discharge voltage.

Additional insight into the frequency response of the CHT may be gained through a comparison with data obtained on SPT geometry thrusters.[7,9,10] In both the CHT and the SPT, there is a transition from relatively low-amplitude oscillations to very strong, large-amplitude oscillations as the discharge voltage is increased. Gascon *et al.*[10] characterized the low-amplitude oscillating regime in SPTs as possessing a broad spectrum of moderate oscillations with a strong peak in the 10-20 kHz range. As the voltage was increased, the SPT entered a regime that contained strong oscillations with multiple harmonics, which is similar to our CHT data. It was also said to be a regime in the SPT where propellant utilization is maximized,[10] which may help to explain the improved efficiency of the CHT[14] when operating at discharge voltages of 250 V and higher. As the propellant flow rate in the CHT is increased (from Fig. 6a to 6c), the relative perturbations in the neutral density that arise from 'breathing' mode oscillations should be reduced. Barral and Ahedo[7] have shown for an SPT that the relative discharge current fluctuations are weakly related to the neutral density fluctuation levels. Without simulations or internal measurements, we can only speculate that this scaling may be sufficient to account for the reduction of current fluctuations with increasing flow rate in the much lower power, lower flow rate CHT.

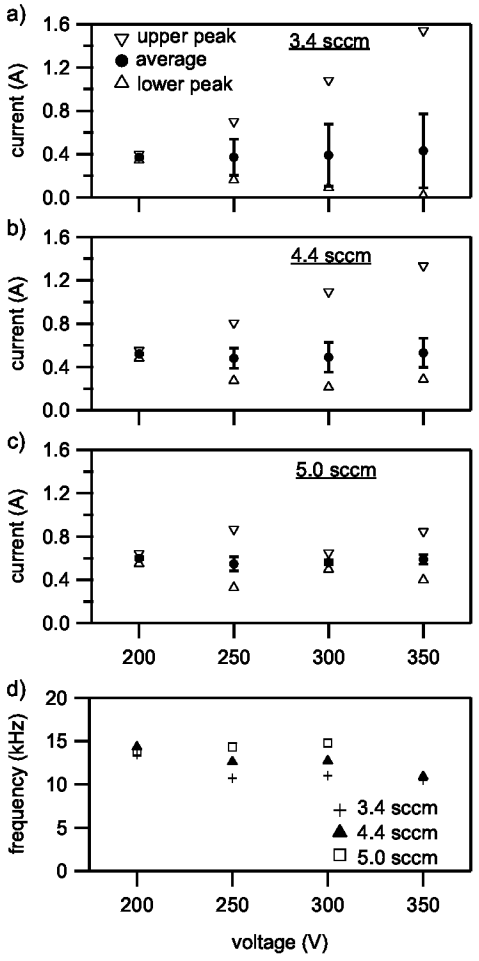

Figure 6. a)-c) Average discharge current as a function of discharge voltage and anode flow rate, shown with the standard deviation of the oscillations (vertical bars) and the minimum and maximum oscillatory current levels. d) Fundamental oscillation frequency as a function of discharge voltage and anode flow rate.

The presence of the strong sharp peak in the frequency spectra of all data in the 11-14 kHz range, coupled with the repeated pattern of current overshoot and starvation illustrated particularly well on the left side of Fig. 3 makes it apparent that this is the so-called 'breathing' mode,[1,15] where the ionization front moves

as neutrals are periodically depleted by enhanced ionization and ion acceleration, and then replenished as additional neutrals stream into the thruster from the anode. This typical instability has been observed in many Hall thrusters, and the standard perturbation analysis leads to a frequency scaling given as[15]

$$\omega = \frac{1}{L}\sqrt{v_i v_n} \tag{1}$$

where L is the characteristic length of the ionization zone and v_i and v_n are the ion and neutral velocities, respectively. For a greater discharge voltage V_d, the ion velocity increases, and if we take L as a constant then the frequency should scale as[10]

$$\omega \sim V_d^{1/4}. \tag{2}$$

Data from SPT-geometries found in Refs. [9, 10] for the most part exhibit this frequency scaling. The fundamental frequencies in the CHT at the various operating points are summarized in Fig. 6d and show that, unlike the scaling given in Eq. (2), the frequency is either unchanged or reduced as the discharge voltage is increased. This could imply that at different voltages the ionization region in the CHT is either not of constant length or is located in a different part of the discharge channel. It could also be that the analysis of the breathing mode, previously performed for an annular Hall thruster possessing a magnetic field that is essentially all in the radial direction, is not adequate for the two-dimensional magnetic field presented by the CHT. One specific point to emphasize is that there is a large axial magnetic field in the CHT, providing a degree of freedom for current-conducting electrons and escaping neutrals not available in the annular geometry SPT with is purely radial field. Another possibility could be that the thruster is in a highly nonlinear oscillatory mode, like that recently predicted for annular Hall thrusters by Barral and Ahedo.[7] In those simulations, the frequency of large-amplitude, nonlinear oscillations are relatively constant as a function of voltage. In rough agreement with these predictions are SPT-100 data presented in Ref. [10], Fig. 5. These data exhibit a reduction in the fundamental frequency as the voltage is increased above 480 V; a scaling that the authors speculated was attributable to nonlinearities not taken into account by the simpler linearized breathing mode model.

The cause of the broad-spectrum oscillations that appear in the 5.0 sccm data below the fundamental frequency of the breathing mode is difficult to identify directly. It could be that in this regime there are multiple ionization regions within the CHT. Alternatively, the ionization region may be tilted with respect to the thruster axis, leading to nonlinearities that produce this second set of observed low-frequency oscillations. A low frequency $\mathbf{E} \times \mathbf{B}$ drift around 3.3 kHz has been observed in the 2.6 cm permanent magnet CHT.[16] This mode does not appear in our data set (discharge current data from that frequency regime were analyzed but didn't exhibit any remarkable features). However, the $\mathbf{E} \times \mathbf{B}$ 'spoke' instability may still be a cause of the slightly higher frequency oscillations observed in the discharge current if tilting of the rotating spoke relative to the thruster yields the observed broad-spectrum oscillations. Another possibility is that the discharge current may oscillate at the observed frequency because of nonlinear interactions and coupling between various plasma modes, which may or may not individually manifest themselves in the current oscillations.

V. Conclusions

Current measurements are used as a way to non-intrusively identify the presence and quantify the importance of various plasma oscillations and instabilities in a cylindrical Hall thruster. The frequency spectra of the discharge current data reveal a rich structure in the low frequency (6-100 kHz) regime; with oscillations generally increasing in magnitude and complexity as the discharge voltage is increased and reducing in severity with increasing flow rate. The data allow for identification of the ionization front instability known as the 'breathing' mode, but the frequency scaling appears to follow a nonlinear scaling instead of the traditional perturbation analysis scaling developed to understand this mode in annular Hall thrusters. At the lowest flowrate, as the discharge voltage is increased a transition from lower amplitude oscillations to large relative fluctuations in the oscillating discharge current is observed. The higher amplitude oscillations are suppressed as the mass flow rate is increased, potentially due to the decrease in the relative fluctuation of neutral atoms in the thruster. A second set of discharge oscillations in the 11-14 kHz range arise at higher propellant flow rates. The source of this set of oscillations is not presently known, but many possibilities involving ionization instabilities and interactions between various oscillations are offered as mechanisms that might excite these modes.

Acknowledgments

Work performed by the Princeton Plasma Physics Laboratory coauthors was partially supported by the U.S. Air Force Office of Scientific Research. We gratefully acknowledge the contributions of MSFC technical support staff Tommy Reid and Doug Galloway, and extend our thanks to students Adam Kimberlin and Joseph Balla for their efforts. We also appreciate and acknowledge the continued MSFC support of Mr. James Martin and Mr. J. Boise Pearson.

References

[1]E.Y. Choueiri, "Plasma oscillations in Hall thrusters," *Phys. Plasmas*, **8**(4):1411, Apr. 2001.

[2]Y. Raitses and N.J. Fisch, "Parametric investigations of a nonconventional Hall thruster," *Phys. Plasmas*, **8**(5):2579, May 2001.

[3]H.R. Kaufman, R.S. Robinson, and R.I. Seddon, "End-Hall ion source," *J. Vac. Sci. Technol. A*, **5**(4):2081, 1987.

[4]A.I. Morozov and V.V. Savel'ev, "Fundamentals of Stationary Plasma Thruster Theory," *Reviews of Plasma Physics*, edited by B.B. Kadomtsev and V.D. Shafranov, Vol. 21, Consultants Bureau, New York, 2000, p. 203.

[5]J. Mueller, "Thruster options for microspacecraft: A review and evaluation of state-of-the-art and emerging technologies," *Micropropulsion for Small Spacecraft*, edited by M.M. Micci and A.D. Ketsdever, Vol. 187, Progress in Astronautics and Aeronautics, AIAA, Reston, VA, 2000, pp. 45-137.

[6]V. Khayms and M. Martinez-Sanchez, "Fifty-watt Hall thruster for microsatellites," *Micropropulsion for Small Spacecraft*, edited by M.M. Micci and A.D. Ketsdever, Vol. 187, Progress in Astronautics and Aeronautics, AIAA, Reston, VA, 2000, pp. 233-254.

[7]S. Barral and E. Ahedo, "Low-frequency model of breathing oscillations in Hall discharges," *Phys. Rev. E*, **79**:046401, 2009.

[8]S. Barral and Z. Peradzyński, "Ionization oscillations in Hall accelerators," (unpublished).

[9]J.-P. Boeuf and L. Garriques, "Low frequency oscillations in a stationary plasma thruster," *J. Appl. Phys.*, **84**(7):3541, 1998.

[10]N. Gascon, M. Dudeck, and S. Barral, "Wall material effects in stationary plasma thrusters. I. Parametric studies of an SPT-100," *Phys. Plasmas*, **10**(10):4123, 2003.

[11]S. Barral, K. Makowski, Z. Peradzyński, N. Gascon, and M. Dudeck, "Wall material effects in stationary plasma thrusters. II. Near-wall and in-wall conductivity," *Phys. Plasmas*, **10**(10):4137, 2003.

[12]K.A. Polzin, T.E. Markusic, B.J. Stanojev, A. Dehoyos, Y. Raitses, A. Smirnov, and N.J. Fisch, "Performance of a Low-Power Cylindrical Hall Thruster," *J. Propuls. Power*, **23**(4):886, 2007.

[13]L. Uribarri and E.Y. Choueiri, "Effects of power supply resonances in onset studies of quasi-steady MPD thrusters," in *43rd AIAA/ASME/SAE/ASEE Joint Propulsion Conference*, July 2007. AIAA Paper 2007-5295.

[14]K.A. Polzin, E.S. Sooby, A.C. Kimberlin, Y. Raitses, E. Merino and N.J. Fisch, "Performance of a permanent-magnet cylindrical Hall-effect thruster," in *45th AIAA/ASME/SAE/ASEE Joint Propulsion Conference*, Aug. 2009. AIAA Paper 2009-4812.

[15]J.M. Fife, M. Martinez-Sanchez, and J. Szabo, "A numerical study of low-frequency discharge oscillations in Hall thrusters," in *33rd AIAA/ASME/SAE/ASEE Joint Propulsion Conference*, July 1997. AIAA Paper 97-3052.

[16]Y. Raitses, E. Merino, J.B. Parker, and N.J. Fisch, "Operation and plume measurements of miniaturized cylindrical Hall thrusters with permanent magnets," in *45th AIAA/ASME/SAE/ASEE Joint Propulsion Conference*, Aug. 2009. AIAA Paper 2009-4810.